LETTER

Magnetostatic chameleonlike metashells with negative permeabilities

To cite this article: L. J. Xu and J. P. Huang 2019 *EPL* **125** 64001

A Letters Journal Exploring the Frontiers of Physics

March 2019

EPL, **125** (2019) 64001 www.epljournal.org
doi: 10.1209/0295-5075/125/64001

Magnetostatic chameleonlike metashells with negative permeabilities

L. J. Xu and J. P. Huang[a]

Department of Physics, State Key Laboratory of Surface Physics, and Key Laboratory of Micro and Nano Photonic Structures (MOE), Fudan University - Shanghai 200433, China

received 5 February 2019; accepted in final form 15 March 2019
published online 26 April 2019

PACS 41.20.Gz – Magnetostatics; magnetic shielding, magnetic induction, boundary-value problems
PACS 51.60.+a – Magnetic properties
PACS 81.05.Zx – New materials: theory, design, and fabrication

Abstract – Magnetic metamaterials have attracted intensive attention for their extraordinary ability to control magnetic fields. However, almost all magnetic metamaterials exhibit no intelligence. This situation largely results from the fact that permeability, as an inherent property, cannot adapt to nearby changes. Inspired by the chameleon behavior, here we design two types of magnetostatic chameleonlike metashells in two dimensions, which are featured by their adaptive responses to inside objects. One type is based on the anisotropic monolayer scheme, and the other is based on the isotropic bilayer scheme. We derive the requirements of magnetostatic chameleonlike metashells by making the effective permeabilities of the chameleonlike metashells always equal to the permeabilities of inside objects. In both schemes, negative permeabilities are required. Theoretical derivations are validated by finite-element simulations. We further extend the anisotropic monolayer scheme to three dimensions. Magnetostatic chameleonlike metashells can act as a type of all-purpose materials to work under different requirements of permeabilities. This work provides intelligence to permeability, and further intelligent metamaterials beyond chameleonlike metashells can be expected.

Introduction. – Magnetic metamaterials [1] have aroused great research interest, such as negative refraction [2,3], magnetic cloak [4–13], magnetic concentrator [14–16], illusion/camouflage [17–22], long-distance transfer and routing [23], magnetic wormhole [24], etc. However, these existing studies on magnetic metamaterials rarely involve intelligence. In other words, once a metamaterial is designed, the function is therewith determined. This situation largely results from the fact that permeability, as an inherent material parameter, lacks adaptivity. In fact, adaptivity is of great significance for practical applications. For example, if the permeability of a magnetic sensor possesses adaptivity, it can always be invisible under different conditions. Therefore, it is urgent to uncover the physics of material adaptivity.

For this purpose, here we propose the concept of magnetostatic chameleonlike metashells which can adaptively change their effective permeabilities according to inside objects. Such behavior is inspired by the natural phenomenon that chameleons can adaptively change their colors according to nearby environments. Concretely speaking, when the designed chameleonlike metashell (fig. 1(a)) is confronted with different inside objects, it can adaptively change its effective permeability to be the same as the permeability of the inside object (the permeability of the matrix is set to be the same as that of the object); see figs. 1(b) and (c). Such behavior is counterintuitive because for a normal shell (fig. 1(d)) it is impossible to exhibit adaptivity; see figs. 1(e) and (f). Note that it is just for convenience to set the matrix property to be the same as the object property. In fact, whatever the matrix property is, the chameleonlike metashell can always imitate the object property and possess the same property as the inside object.

To uncover the physics of magnetostatic chameleonlike metashells, we calculate the effective permeabilities of the core-shell structure and the core-shell-shell structure, which respectively serve as the anisotropic monolayer

[a]E-mail: jphuang@fudan.edu.cn

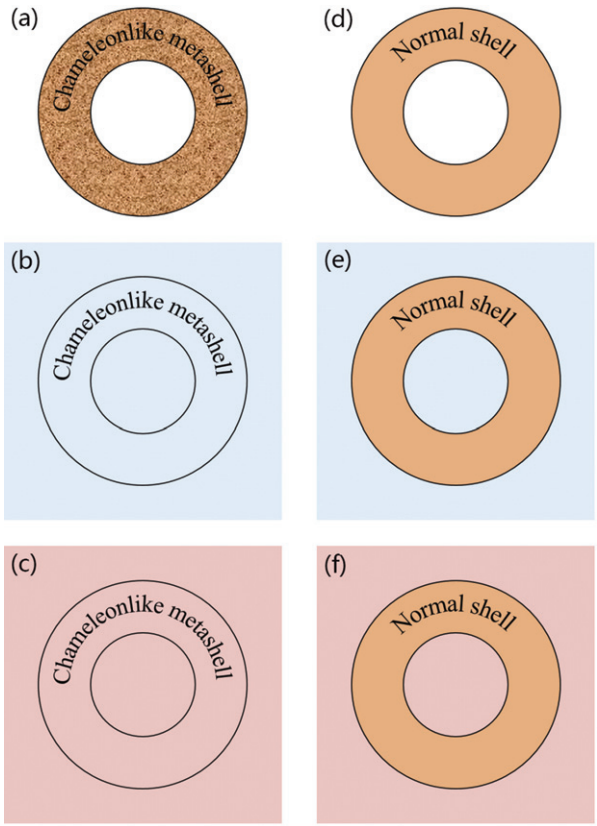

Fig. 1: Schematic diagrams of (a)–(c) chameleonlike metashells *vs.* (d)–(f) normal shells. Different colors represent different permeabilities.

scheme and the isotropic bilayer scheme. We find some special relations to make the effective permeabilities of chameleonlike metashells be the same as the permeabilities of inside objects. In what follows, we will perform theoretical derivation and finite-element simulations to validate the proposed schemes. To be mentioned, "permeability" in this work represents "relative permeability", say regarding vacuum permeability as 1.

Theory for chameleonlike metashells. – The key to magnetostatic chameleonlike metashells is their adaptive permeabilities according to inside objects. Therefore, we will start from deriving the effective permeabilities in two dimensions to uncover the physics of magnetostatic chameleonlike metashells. For this realization, we will firstly consider an anisotropic monolayer scheme; see fig. 2(a). Due to the fact that anisotropy is not that easy to obtain in experiments, we will further discuss an isotropic bilayer scheme; see fig. 2(c), to simplify the parameters. In both schemes, negative permeabilities are required. Although negative permeabilities do not exist in nature, they can be realized with manually fabricated structures [25–29]. Especially in a recent work [29], negative permeabilities are experimentally obtained by an appropriately tailored set of currents. Concretely speaking, surface currents are externally applied on both the inner

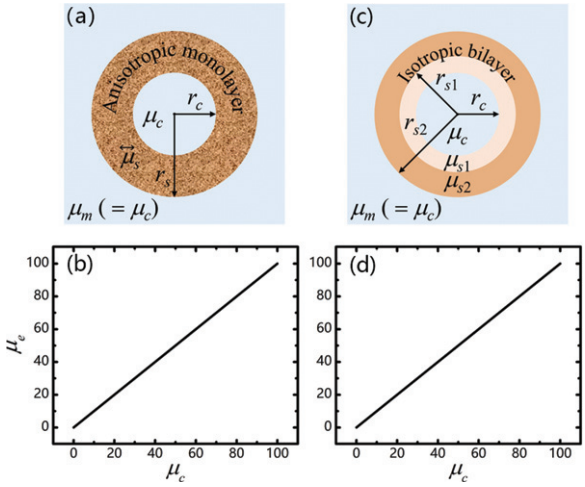

Fig. 2: Schematic diagrams of (a) an anisotropic monolayer scheme and (c) an isotropic bilayer scheme. (b) and (d) are theoretical results with respect to eqs. (4) and (7).

and outer surfaces of the shell to make the shell possess negative permeability. Similar approach may also be applied in this work to realize negative permeabilities.

Anisotropic monolayer scheme. We consider the core-shell structure in fig. 2(a). We set the core with radius r_c and scalar permeability μ_c, and the shell with radius r_s and tensorial permeability $\mu_s = \mathrm{diag}\,(\mu_{rr}, \mu_{\theta\theta})$ in cylindrical coordinates (r, θ). It should be noted that $\mu_{\theta\theta}/\mu_{rr} < 0$. We can derive the effective permeability of the core-shell structure μ_e as

$$\mu_e = m\mu_{rr}\frac{\mu_c + m\mu_{rr}\tan\left(m\ln\sqrt{p}\right)}{m\mu_{rr} - \mu_c\tan\left(m\ln\sqrt{p}\right)}, \tag{1}$$

where $m = \sqrt{-\mu_{\theta\theta}/\mu_{rr}}$, and $p = (r_c/r_s)^2$ is the core fraction. Detailed derivation can be found in the first subsection of the appendix.

As the definition suggests, magnetostatic chameleonlike metashells possess adaptive responses to inside objects. In other words, the effective scalar permeabilities of the metashells (μ_s) are always equal to the permeabilities of inside objects,

$$\mu_s = \mu_c. \tag{2}$$

Due to the requirement of eq. (2), the effective permeability of the core-shell structure (μ_e) can then be expressed as

$$\mu_e = \mu_c. \tag{3}$$

In this way, the question is to find some special relations to make eq. (1) turn into eq. (3). Fortunately, we find a special relation

$$\sqrt{-\mu_{\theta\theta}/\mu_{rr}}\ln\sqrt{p} = -Z^+\pi, \tag{4}$$

where $Z^+ (= 1, 2, 3, \cdots)$ can be any positive integer. Clearly, with eq. (4), the requirement of eq. (3) is perfectly satisfied; see fig. 2(b). In the anisotropic monolayer

scheme, the size of the chameleonlike metashell is not restricted because we can adjust another two variations, say μ_{rr} and $\mu_{\theta\theta}$. Note that such scheme can be extended to three dimensions, and details can be found in the second subsection of the appendix.

Isotropic bilayer scheme. Then we consider the core-shell-shell structure in fig. 2(c). We set the core with radius r_c and scalar permeability μ_c, and the two shells with radius r_{s1}, r_{s2} and scalar permeabilities μ_{s1}, μ_{s2}. We can derive the effective permeability of the core-shell-shell structure μ_e as [30]

$$\mu_e = \mu_{s2}\frac{\mu_{12}+\mu_{s2}+(\mu_{12}-\mu_{s2})\,p_{12}}{\mu_{12}+\mu_{s2}-(\mu_{12}-\mu_{s2})\,p_{12}}, \tag{5}$$

where $p_{12} = (r_{s1}/r_{s2})^2$. μ_{12} is the effective permeability of the core plus the first shell, which can be calculated as [30]

$$\mu_{12} = \mu_{s1}\frac{\mu_c+\mu_{s1}+(\mu_c-\mu_{s1})\,p_c}{\mu_c+\mu_{s1}-(\mu_c-\mu_{s1})\,p_c}, \tag{6}$$

where $p_c = (r_c/r_{s1})^2$.

Fortunately, we also find a special relation to make eq. (5) turn into eq. (3),

$$(\mu_{s1}+\mu_{s2})^2 + (p_c - p_{12})^2 = 0. \tag{7}$$

Namely, $\mu_{s1}+\mu_{s2}=0$ and $p_c - p_{12}=0$ should be simultaneously satisfied. Clearly, with eq. (7), the requirement of eq. (3) is perfectly satisfied; see fig. 2(d). In the isotropic bilayer scheme, the size of the chameleonlike metashell is restricted to be $p_c = p_{12}$. It should be noted that such scheme cannot be extended to three dimensions, which will be explained in the third subsection of the appendix.

So far, we have uncovered the physics of magnetostatic chameleonlike metashells in two dimensions, say eq. (4) for the anisotropic monolayer scheme and eq. (7) for the isotropic bilayer scheme. Next we will perform finite-element simulations to validate the two proposed schemes with COMSOL Multiphysics (`http://www.comsol.com/`).

Simulation for chameleonlike metashells. – The metashells are featured by their adaptive responses to inside objects. Normal shells are applied to demonstrate that common materials do not possess adaptivity. Comparative shells with the same permeabilities of inside objects are applied to compare with chameleonlike metashells. If the magnetic scalar potential distributions outside the comparative shell and chameleonlike metashell are the same, the chameleonlike metashell does work as expected. For simplicity, the permeabilities of matrices are set to be the same as those of objects.

Anisotropic monolayer scheme. According to eq. (4), we design the chameleonlike metashell with the anisotropic monolayer scheme; see figs. 3(a)–(d). We take figs. 3(a), (e), and (i) as an example to make the finite-element simulations understandable. When the permeability of the inside object is 1; see fig. 3(a), the chameleonlike metashell

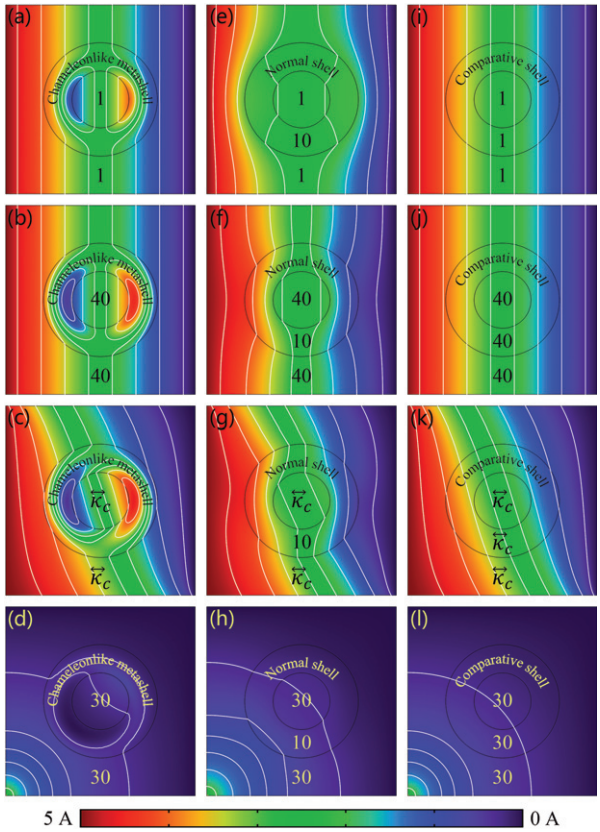

Fig. 3: Finite-element simulations of the anisotropic monolayer scheme. The size of simulation box is 10×10 cm, $r_c = 1.5$ cm and $r_s = 3$ cm for (a)–(l). For the first three rows, the magnetic scalar potentials are 5 A for the left boundary, 0 A for the right one, and insulated for the others. For the last row, the magnetic scalar potentials are 5 A for the lower left point, 0 A for the upper and right ones, and insulated for the others. The permeabilities of chameleonlike metashells and normal shells are respectively diag $(10, -205.42)$ in cylindrical coordinates (designed according to eq. (4)) and 10. The other permeabilities in each simulation box are 1 for (a), (e), and (i), 40 for (b), (f), and (j), $((45, -25), (-25, 45))$ in Cartesian coordiantes for (c), (g), and (k), and 30 for (d), (h), and (l). White lines represent equipotential lines.

adaptively changes its effective permeability to be 1, which results in the same matrix potential distribution as that in fig. 3(i). However, the normal shell in fig. 3(e) fails to change its permeability adaptively, which results in the different matrix potential distribution from that in fig. 3(i). Then we change the permeability of the object to be 40; see figs. 3(b), (f), and (j). The same matrix potential distributions between figs. 3(b) and (j) demonstrate that the chameleonlike metashell works, whereas the different matrix potential distributions between figs. 3(f) and (j) illustrate that the normal shell fails.

Then we extend the anisotropic monolayer scheme by setting the permeability of the object to be anisotropic; see figs. 3(c), (g), and (k), and exposing the device into a nonuniform external field; see figs. 3(d), (h), and (l).

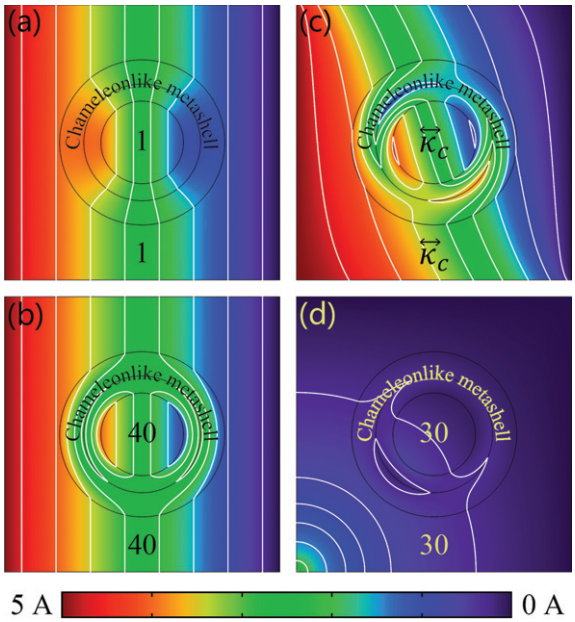

Fig. 4: Finite-element simulations of the isotropic bilayer scheme. The parameters of (a)–(d) are the same as those in figs. 3(a)–(d) except for the chameleonlike metashell. Namely, $\mu_{s1} = -10$, $\mu_{s2} = 10$, $r_c = 1.5\,\mathrm{cm}$, $r_{s1} = 3\sqrt{2}/2\,\mathrm{cm}$, and $r_{s2} = 3\,\mathrm{cm}$, which are designed according to eq. (7).

The results show that the chameleonlike metashell is robust under more complicated conditions. Note that the permeabilities of objects like 30 and 40 can correspond to practical materials like ferromagnetic materials iron, steel, etc.

Isotropic bilayer scheme. According to the requirement of eq. (7), we also design the chameleonlike metashell with the isotropic bilayer scheme; see figs. 4(a)–(d). For the convenience of comparison, we perform the finite-element simulations based on the same parameters in figs. 3(a)–(d) except for the chameleonlike metashell, and hence we obtain figs. 4(a)–(d). Clearly, the same matrix potential distributions between figs. 4(a)–(d) and figs. 3(a)–(d) demonstrate that the isotropic bilayer scheme can achieve the same effects as anisotropic monolayer scheme.

In a word, the chameleonlike metashells experience no manual changes in figs. 3(a)–(d) and figs. 4(a)–(d), but they exhibit adaptive responses to inside objects, which is the key point of this work.

Discussion and conclusion. – When deriving the requirement of the anisotropic monolayer scheme (eq. (4)), we refer to the previous work on calculating the effective permeability with negative value [29,30]. When deriving the requirement of the isotropic bilayer scheme (eq. (7)), the idea is, to some extent, related to partially resonant composites [31–35].

Compared with the anisotropic monolayer scheme, the isotropic bilayer scheme may be more feasible for practical application because anisotropy is really difficult to achieve especially for the fact that the two components of the anisotropic tensor are one positive and one negative. In fact, although an exact chameleonlike metashell cannot be achieved with all positive permeabilities, an approximate one can be realized with all positive permeabilities. The related mechanism has been revealed in electrostatics [36]. Another problem is that negative permeabilities may result in a large loss. When considering the loss, the results will be very different because here we only discuss the magnetostatic field where loss does not exist.

Moreover, an unexpected phenomenon should be noticed, *i.e.*, that the isotropic bilayer scheme cannot be extended to three dimensions. Such situation, from another perspective, just proves the indispensability and specificity of the anisotropic monolayer scheme.

The potential application of magnetostatic chameleonlike metashells is to act as a type of all-purpose materials. Concretely speaking, they can meet different requirements of permeabilities under different conditions.

In summary, we have proposed two schemes to design magnetostatic chameleonlike metashells in two dimensions. Theoretical derivations and finite-element simulations both validate the feasibility. Furthermore, we succeed in extending the anisotropic monolayer scheme to three dimensions. This work lays the foundation for magnetostatic chameleonlike metashells, and may provide guidance for exploring intelligent metamaterials not only in magnetostatics, but also in other disciplines like thermotics and electrostatics.

* * *

We acknowledge the financial support by the National Natural Science Foundation of China under Grant No. 11725521.

Appendix. –

Details for deriving eq. (1). The dominant equation in magnetostatics is

$$\boldsymbol{\nabla} \cdot (-\mu \boldsymbol{\nabla} \varphi) = 0, \tag{A.1}$$

where μ and φ are, respectively, tensorial permeability and magnetic scalar potential.

Equation (A.1) can be expanded in cylindrical coordinates as

$$\frac{\partial}{\partial r}\left(r\mu_{rr}\frac{\partial \varphi}{\partial r}\right) + \frac{\partial}{\partial \theta}\left(\mu_{\theta\theta}\frac{\partial \varphi}{r\partial \theta}\right) = 0. \tag{A.2}$$

The general solution of eq. (A.2) is

$$\begin{aligned}\varphi\left(\mu_{\theta\theta}/\mu_{rr} < 0\right) &= A_0 + B_0 \ln r \\ &+ \sum_{i=1}^{\infty}\left[A_i \sin\left(i\theta\right) + B_i \cos\left(i\theta\right)\right]\sin\left(im\ln r\right) \\ &+ \sum_{i=1}^{\infty}\left[C_i \sin\left(i\theta\right) + D_i \cos\left(i\theta\right)\right]\cos\left(im\ln r\right), \end{aligned} \tag{A.3}$$

$$\varphi\left(\mu_{\theta\theta}/\mu_{rr}>0\right)=E_0+F_0\ln r+\sum_{i=1}^{\infty}\left[E_i\sin\left(i\theta\right)+F_i\cos\left(i\theta\right)\right]r^{in}+\sum_{i=1}^{\infty}\left[G_i\sin\left(i\theta\right)+H_i\cos\left(i\theta\right)\right]r^{-in},\tag{A.4}$$

where $m=\sqrt{-\mu_{\theta\theta}/\mu_{rr}}$, and $n=\sqrt{\mu_{\theta\theta}/\mu_{rr}}$.

The magnetic scalar potential distributions of the core (φ_c), shell (φ_s), and matrix (φ_m) can then be determined by the following boundary conditions:

$$\begin{cases}\varphi_c<\infty,\\ \varphi_c\left(r_c\right)=\varphi_s\left(r_c\right),\\ \varphi_s\left(r_s\right)=\varphi_m\left(r_s\right),\\ \left(-\mu_c\partial\varphi_c/\partial r\right)_{r_c}=\left(-\mu_{rr}\partial\varphi_s/\partial r\right)_{r_c},\\ \left(-\mu_{rr}\partial\varphi_s/\partial r\right)_{r_s}=\left(-\mu_m\partial\varphi_m/\partial r\right)_{r_s},\\ \boldsymbol{\nabla}\varphi_m\left(r\to\infty\right)=\boldsymbol{\nabla}\varphi_0,\end{cases}\tag{A.5}$$

where $\boldsymbol{\nabla}\varphi_0$ represents the external uniform potential gradient.

For the symmetric boundary conditions of eq. (A.5), we only require to keep several terms with $i=1$ in eq. (A.3) and (A.4),

$$\varphi\left(\mu_{\theta\theta}/\mu_{rr}<0\right)=A_0+B_1\cos\theta\sin\left(m\ln r\right)+D_1\cos\theta\cos\left(m\ln r\right),\tag{A.6}$$

$$\varphi\left(\mu_{\theta\theta}/\mu_{rr}>0\right)=E_0+F_1r^n\cos\theta+H_1r^{-n}\cos\theta.\tag{A.7}$$

Therefore, for isotropic matrix, we can obtain $\varphi_m=E_0+F_1r\cos\theta+H_1r^{-1}\cos\theta$. We set H_1 to be zero to ensure the external field to be undistorted. Then we can derive the effective permeability of the core-shell structure μ_e as eq. (1).

Three-dimensional counterpart of anisotropic monolayer scheme. Equation (A.1) can be expanded in spherical coordinates as

$$\frac{1}{r}\frac{\partial}{\partial r}\left(r^2\mu_{rr}\frac{\partial\varphi}{\partial r}\right)+\frac{1}{\sin\theta}\frac{\partial}{\partial\theta}\left(\sin\theta\mu_{\theta\theta}\frac{\partial\varphi}{r\partial\theta}\right)=0.\tag{A.8}$$

The general solution of eq. (A.8) is

$$\varphi\left(\mu_{\theta\theta}/\mu_{rr}<-1/8\right)=A_0+B_0r^{-1}+\sum_{i=1}^{\infty}r^{-1/2}\left[A_i\sin\left(s\ln r\right)+B_i\cos\left(s\ln r\right)\right]\times P_i\left(\cos\theta\right),\tag{A.9}$$

$$\varphi\left(-1/8<\mu_{\theta\theta}/\mu_{rr}<0\right)=C_0+D_0r^{-1}+\sum_{i=1}^{j}\left(C_ir^{t_1}+D_ir^{t_2}\right)P_i\left(\cos\theta\right)+\sum_{i=j+1}^{\infty}r^{-1/2}\left[E_i\sin\left(s\ln r\right)+F_i\cos\left(s\ln r\right)\right]\times P_i\left(\cos\theta\right),\tag{A.10}$$

$$\varphi\left(0\le\mu_{\theta\theta}/\mu_{rr}\right)=G_0+H_0r^{-1}+\sum_{i=1}^{\infty}\left(G_ir^{t_1}+H_ir^{t_2}\right)P_i\left(\cos\theta\right),\tag{A.11}$$

where $s=\sqrt{-1/4-i\left(i+1\right)\mu_{\theta\theta}/\mu_{rr}}$, $t_{1,2}=-1/2\pm\sqrt{1/4+i\left(i+1\right)\mu_{\theta\theta}/\mu_{rr}}$, i is the summation index, $j=\mathrm{INT}[-1/2+\sqrt{1/4-\mu_{rr}/\left(4\mu_{\theta\theta}\right)}]$, and $\mathrm{INT}\left[\cdots\right]$ is the integral function with respect to $\cdots$. P_i is Legendre polynomials.

We find that eqs. (A.10) and (A.11) are essentially the same with similar boundary conditions of eq. (A.5), for we only require to keep several terms of $i=1$, and hence eqs. (A.9)–(A.11) can be simplified as

$$\varphi\left(\mu_{\theta\theta}/\mu_{rr}<-1/8\right)=A_0+r^{-1/2}\left[A_1\sin\left(u\ln r\right)+B_1\cos\left(u\ln r\right)\right]\cos\theta,\tag{A.12}$$

$$\varphi\left(\mu_{\theta\theta}/\mu_{rr}>-1/8\right)=G_0+\left(G_1r^{v_1}+H_1r^{v_2}\right)\cos\theta,\tag{A.13}$$

where $u=\sqrt{-1/4-2\mu_{\theta\theta}/\mu_{rr}}$, and $t_{1,2}=-1/2\pm\sqrt{1/4+2\mu_{\theta\theta}/\mu_{rr}}$,

We set the core with radius r_c and scalar permeability μ_c, and the shell with radius r_s and tensorial permeability $\mu_s=\mathrm{diag}\left(\mu_{rr},\,\mu_{\theta\theta},\,\mu_{\varphi\varphi}\right)$ with $\mu_{\theta\theta}=\mu_{\varphi\varphi}$ for brevity. It should be noted that $\mu_{\theta\theta}/\mu_{rr}<-1/8$.

For the isotropic matrix, we can obtain $\varphi_m=G_0+\left(G_1r+H_1r^{-2}\right)\cos\theta$. We set H_1 to be zero to ensure the external field to be undistorted. Then we can derive the effective permeability of the core-shell structure μ_e in three dimensions as

$$\mu_e=\mu_{rr}\frac{4u\mu_c+\left[2\mu_c+\left(1+4u^2\right)\mu_{rr}\right]\tan\left(u\ln\sqrt[3]{p}\right)}{4u\mu_{rr}-2\left(2\mu_c+\mu_{rr}\right)\tan\left(u\ln\sqrt[3]{p}\right)},\tag{A.14}$$

where $p=\left(r_c/r_s\right)^3$ is the core fraction.

Fortunately, we find a special relation to make eq. (A.14) satisfy the requirement of eq. (3)

$$\sqrt{-1/4-2\mu_{\theta\theta}/\mu_{rr}}\ln\sqrt[3]{p}=-Z^+\pi,\tag{A.15}$$

where $Z^+(=1,2,3,\ldots)$ can be any positive integer. Clearly, with eq. (A.15), the requirement of eq. (3) is perfectly satisfied. Therefore, magnetostatic chameleonlike metshells can be achieved in three dimensions with anisotropic monolayer scheme.

Explanation for the failure of the three-dimensional isotropic bilayer scheme. We consider the core-shell-shell structure in three dimensions. We set the core with radius r_c and scalar permeability μ_c, and the two shells

with radius r_{s1}, r_{s2} and scalar permeabilities μ_{s1}, μ_{s2}. We can derive the effective permeability of the core-shell-shell structure μ_e as [30]

$$\mu_e = \mu_{s2}\frac{\mu_{12} + 2\mu_{s2} + 2\left(\mu_{12} - \mu_{s2}\right)p_{12}}{\mu_{12} + 2\mu_{s2} - \left(\mu_{12} - \mu_{s2}\right)p_{12}}, \tag{A.16}$$

where $p_{12} = \left(r_{s1}/r_{s2}\right)^3$. μ_{12} is the effective permeability of the core plus the first shell, which can be calculated as [30]

$$\mu_{12} = \mu_{s1}\frac{\mu_c + 2\mu_{s1} + 2\left(\mu_c - \mu_{s1}\right)p_c}{\mu_c + 2\mu_{s1} - \left(\mu_c - \mu_{s1}\right)p_c}, \tag{A.17}$$

where $p_c = \left(r_c/r_{s1}\right)^3$.

Although we find a special relation to make eq. (A.16) turn into eq. (3),

$$\left[\left(p_{12} - 2p_c + p_c p_{12}\right)\mu_c - \left(p_c - 2p_{12} + p_c p_{12}\right)\mu_{s1}\right]^2 + \left(\mu_{s1} + 2\mu_{s2}\right)^2 = 0, \tag{A.18}$$

eq. (A.18) is dependent on μ_c. Therefore, the isotropic bilayer scheme cannot work as magnetostatic chameleonlike metshells in three dimensions.

REFERENCES

[1] Magnus F., Wood B., Moore J., Morrison K., Perkins G., Fyson J., Wiltshire M. C. K., Caplin D., Cohen L. F. and Pendry J. B., *Nat. Mater.*, **7** (2008) 295.

[2] Liu S. Y., Chen W. K., Du J. J., Lin Z. F., Chui S. T. and Chan C. T., *Phys. Rev. Lett.*, **101** (2008) 157407.

[3] Gao Y., Huang J. P., Liu Y. M., Gao L., Yu K. W. and Zhang X., *Phys. Rev. Lett.*, **104** (2010) 034501.

[4] Sanchez A., Navau C., Prat-Camps J. and Chen D. X., *New J. Phys.*, **13** (2011) 093034.

[5] Gomory F., Solovyov M., Souc J., Navau C., Prat-Camps J. and Sanchez A., *Science*, **335** (2012) 1466.

[6] Narayana S. and Sato Y., *Adv. Mater.*, **24** (2012) 71.

[7] Souc J., Solovyov M., Gomory F., Prat-Camps J., Navau C. and Sanchez A., *New J. Phys.*, **15** (2013) 053019.

[8] Wang R. F., Mei Z. L., Yang X. Y., Ma X. and Cui T. J., *Phys. Rev. B*, **89** (2014) 165108.

[9] Yampolskii S. V. and Genenko Y. A., *Appl. Phys. Lett.*, **104** (2014) 033501.

[10] Zhu J. F., Jiang W., Liu Y. C., Yin G., Yuan J., He S. L. and Ma Y. G., *Nat. Commun.*, **6** (2015) 8931.

[11] Solovyov M., Souc J. and Gomory F., *IEEE Trans. Appl. Supercond.*, **25** (2015) 1.

[12] Jiang W., Ma Y. G., Zhu J. F., Yin G., Liu Y. C., Yuan J. and He S. L., *NPG Asia Mater.*, **9** (2017) e341.

[13] Jiang W., Ma Y. G. and He S. L., *Phys. Rev. Appl.*, **9** (2018) 054041.

[14] Navau C., Prat-Camps J. and Sanchez A., *Phys. Rev. Lett.*, **109** (2012) 263903.

[15] Sun F. and He S. L., *Prog. Electromagn. Res.*, **142** (2013) 579.

[16] Prat-Camps J., Sanchez A. and Navau C., *Supercond. Sci. Technol.*, **26** (2013) 074001.

[17] Sun F. and He S. L., *Sci. Rep.*, **4** (2014) 6593.

[18] Mach-Batlle R., Navau C. and Sanchez A., *Appl. Phys. Lett.*, **112** (2018) 162406.

[19] Mach-Batlle R., Parra A., Laut S., Del-Valle N., Navau C. and Sanchez A., *Phys. Rev. Appl.*, **9** (2018) 034007.

[20] Han T. C., Bai X., Thong J. T. L., Li B. W. and Qiu C. W., *Adv. Mater.*, **26** (2014) 1731.

[21] Yang T. Z., Bai X., Gao D. L., Wu L. Z., Li B. W., Thong J. T. L. and Qiu C. W., *Adv. Mater.*, **27** (2015) 7752.

[22] Han T. C. and Qiu C. W., *J. Opt.*, **18** (2016) 044003.

[23] Navau C., Prat-Camps J., Romero-Isart O., Cirac J. I. and Sanchez A., *Phys. Rev. Lett.*, **112** (2014) 253901.

[24] Prat-Camps J., Navau C. and Sanchez A., *Sci. Rep.*, **5** (2015) 12488.

[25] Veselago V. G., *Sov. Phys. Usp.*, **10** (1968) 509.

[26] Dolgov O. V., Kirzhnits D. A. and Losyakov V. V., *Solid State Commun.*, **46** (1983) 147.

[27] Pendry J. B., Holden A. J., Robbins D. J. and Stewart W. J., *IEEE Trans. Microwave Theory Tech.*, **47** (1999) 2075.

[28] Alu A., Salandrino A. and Engheta N., *Opt. Express*, **14** (2006) 1557.

[29] Mach-Batlle R., Parra A., Prat-Camps J., Laut S., Navau C. and Sanchez A., *Phys. Rev. B*, **96** (2017) 094422.

[30] Jin J. F., Liu S. Y., Lin Z. F. and Chui S. T., *Phys. Rev. B*, **80** (2009) 115101.

[31] Nicorovici N. A. and McPhedran R. C., *Phys. Rev. B*, **49** (1994) 8479.

[32] Levy O., *J. Appl. Phys.*, **77** (1995) 1696.

[33] Liu X. Y. and Li Z. Y., *Phys. Lett. A*, **223** (1996) 475.

[34] Milton G. W. and Nicorovici N. A. P., *Proc. R. Soc. Lond. A.*, **462** (2006) 3027.

[35] Yu X. P. and Gao L., *Phys. Lett. A*, **359** (2006) 516.

[36] Xu L. J. and Huang J. P., *Eur. Phys. J. B*, **92** (2019) 53.